ACADEMIC PRESS

Available online at www.sciencedirect.com

SCIENCE DIRECT®

Journal of Sound and Vibration 266 (2003) 171–187

JOURNAL OF SOUND AND VIBRATION

www.elsevier.com/locate/jsvi

# Generation of elastic waves in a laminated solid by a moving photothermal source

A. Kononov*, R. de Borst

*Faculty of Aerospace Engineering, Engineering Mechanics, Koiter Institute Delft, P.O. Box 5058, 2600 GB Delft, The Netherlands*

Received 4 April 2002; accepted 9 September 2002

**Abstract**

The steady state response of an elastic layered plate (laminate) which is subjected to a moving laser source illumination is studied. The response of the laminate is obtained using the transfer matrix approach. The application of the photo-thermal source (laser) to the upper surface of the laminate is formulated as equivalent stresses applied at the illuminated boundary. The equivalent stresses are derived with the use of the causality principle. It is shown that the generated displacement field is sensitive to the variations of the laminate inner structure and also to the variations of the elastic properties of a bonded elastic half-space.


## 1. Introduction

The past two decades have witnessed an intensive research in *laser acoustics*. This is an interdisciplinary area which was originated in collaboration between researchers from acoustics, quantum electronics and integral optics. By bringing lasers into acoustics and non-destructive material evaluation (NDE), many useful techniques have been designed, e.g., new sound transducers and receivers and optical data processing [1]. In particular, pulsed laser sources may generate wide-bandwidth acoustic signals, thus providing a new method for non-destructive, non-contact material evaluation [2,3].

Many papers are devoted to the analysis of laser-generated ultrasound in a half-space or in thin plates [4–6]. The majority of the papers are related to pulse propagation, which arises due to a short laser pulse applied at the same area of a solid. In the present paper, an acoustic field is

*Corresponding author. Tel.: +0031-15-278-5460; fax: +0031-15-2611465.
*E-mail address:* a.kononov@lr.tudelft.nl (A. Kononov).

0022-460X/03/$ - see front matter 
doi:10.1016/S0022-460X(02)01565-1

considered which is generated by a laser beam which uniformly scans over the surface of a laminated solid. The power intensity of the laser beam is assumed to be harmonically modulated.

The ultrasound generation by a moving photothermal source in a fluid has previously been addressed, see for example an extended review in Ref. [7], or in Ref. [8]. However, for solids (especially for laminated solids) this problem has not been studied. The major advantage of a moving photothermal source is that the characteristics of the acoustic field generated by a moving source can be adjusted either by changing the modulation frequency of the laser beam or by changing the velocity of the laser spot motion over the specimen surface. The most effective adjustment of the acoustic field characteristics can be achieved by choosing the proper law of motion of the photothermal source, since the directivity and the frequency spectrum of the radiation are defined by the law of source motion.

The response of the laminated solid in the Fourier domain is obtained using the transfer matrix approach [9,10]. This approach with some modifications depending on the situation appears to be a standard procedure for such problems.

## 2. Problem statement

Consider a multi-layered elastic solid, which consists of $n$ planar homogeneous and isotropic elastic layers, with thickness $h_j$ ($j = 1, \ldots, n$). The upper surface of the laminate is subjected to laser pulse illumination, as depicted in Fig. 1.

The origin of the co-ordinate system is placed at the lower boundary of the bottom layer and the total thickness of the entire laminate is denoted by $H$. As will be shown later, the laser or photothermal source may be represented as an equivalent elastic boundary source consisting of distributed normal and shear loading boundary conditions. Accordingly, only a purely mechanical load will initially be considered (no thermo-effects).

Consider an elastic layer with number $l$. In Cartesian co-ordinates and in the absence of body forces, the displacement vector of the elastic media, **u**, can be represented in terms of three scalar

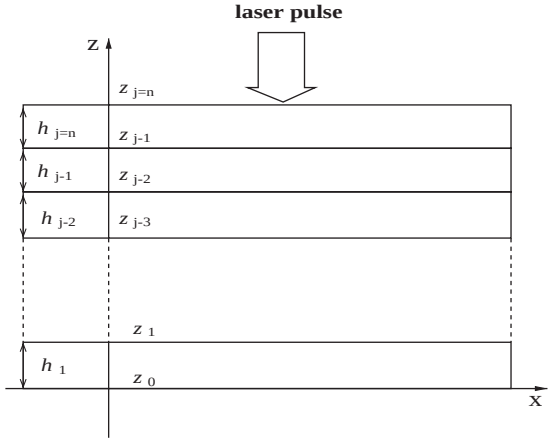


Fig. 1. Model and reference system.

potentials [11],

$$\mathbf{u} = \boldsymbol{\nabla}\phi + \boldsymbol{\nabla} \times \psi_1 \mathbf{e}_z + \boldsymbol{\nabla} \times \boldsymbol{\nabla} \times \psi_2 \mathbf{e}_z, \tag{1}$$

where $\mathbf{e}_z$ is the unit vector in the direction of $z$-axis, and $\phi(x, y, z, t)$, $\psi_1(x, y, z, t)$, $\psi_2(x, y, z, t)$ are scalar potentials. Then, the equations of elasticity reduce to the following equations for the potentials:

$$\boldsymbol{\nabla}^2\phi - \frac{1}{a^2}\frac{\partial^2\phi}{\partial t^2} = 0, \quad \boldsymbol{\nabla}^2\psi_\varepsilon - \frac{1}{b^2}\frac{\partial^2\psi_\varepsilon}{\partial t^2} = 0, \quad \varepsilon = 1, 2, \tag{2}$$

where $a = \sqrt{(\lambda + 2\mu)/\rho}, b = \sqrt{\mu/\rho}$ are the velocities of the compressional and shear waves written in terms of the Lamé constants $\lambda$ and $\mu$ and the mass density $\rho$. Using Eq. (1) and the following stress–displacement relations

$$\sigma_{zz} = 2\mu\frac{\partial u_z}{\partial z} + \lambda\nabla.\mathbf{u}, \tau_{xz} = \mu\left(\frac{\partial u_x}{\partial z} + \frac{\partial u_z}{\partial x}\right), \tau_{yz} = \mu\left(\frac{\partial u_y}{\partial z} + \frac{\partial u_z}{\partial y}\right),$$

the stresses can be expressed in terms of the potentials as follows:

$$\begin{aligned}
\sigma_{zz} &= \frac{\lambda}{a^2}\frac{\partial^2\phi}{\partial t^2} + 2\mu\left(\frac{\partial^2\phi}{\partial z^2} + \frac{\partial^3\psi_2}{\partial z^3}\right) - 2\rho\frac{\partial^3\psi_2}{\partial z\partial t^2},\\
\tau_{xz} &= 2\mu\left(\frac{\partial^2\phi}{\partial z\partial x} + \frac{\partial^3\psi_2}{\partial x\partial z^2}\right) + \mu\frac{\partial^2\psi_1}{\partial z\partial y} - \rho\frac{\partial^3\psi_2}{\partial x\partial t^2},\\
\tau_{yz} &= 2\mu\left(\frac{\partial^2\phi}{\partial z\partial y} + \frac{\partial^3\psi_2}{\partial y\partial z^2}\right) - \mu\frac{\partial^2\psi_1}{\partial z\partial x} - \rho\frac{\partial^3\psi_2}{\partial y\partial t^2}.
\end{aligned} \tag{3}$$

In Eqs. (2) and (3), $a$, $b$, $\mu$, $\lambda$ and $\rho$ refer to the particular layer. Inside the laminate the stress tensor and displacement vector have to be continuous across the boundaries of the layers, so that the following relations at each layer-to-layer interface are valid:

$$\begin{aligned}
&\mathbf{u}^{(j)}(x, y, z = z_{j-1}, t) = \mathbf{u}^{(j-1)}(x, y, z = z_{j-1}, t), \quad j = 1, \ldots, n,\\
&\sigma_{zz}^{(j)} = \sigma_{zz}^{(j-1)}, \tau_{xz}^{(j)} = \tau_{xz}^{(j-1)}, \tau_{yz}^{(j)} = \tau_{yz}^{(j-1)}.
\end{aligned} \tag{4}$$

Application of a Fourier transform over the time and plane spatial co-ordinates

$$\tilde{F}(k_1, k_2, z, \omega) = \int\int\int F(x, y, z, t)\mathrm{e}^{\mathrm{i}(\omega t - k_1 x - k_2 y)}\,\mathrm{d}x\,\mathrm{d}y\,\mathrm{d}t, \tag{5}$$

to Eqs. (2) results in a set of ordinary differential equations with respect to the $z$-co-ordinate:

$$\frac{\partial^2\tilde{\phi}}{\partial z^2} + \alpha^2\tilde{\phi} = 0, \quad \frac{\partial^2\tilde{\psi}_\varepsilon}{\partial z^2} + \beta^2\tilde{\psi}_\varepsilon = 0, \quad \varepsilon = 1, 2 \tag{6}$$

with corresponding general solutions in terms of up- and down-going waves inside the layer

$$\begin{aligned}
&\tilde{\phi} = A_1\mathrm{e}^{\mathrm{i}\alpha(z - z_{l-1})} + A_2\mathrm{e}^{-\mathrm{i}\alpha(z - z_{l-1})}, \quad z_{l-1} \leqslant z \leqslant z_l,\\
&\tilde{\psi}_1 = B_1\mathrm{e}^{\mathrm{i}\beta(z - z_{l-1})} + B_2\mathrm{e}^{-\mathrm{i}\beta(z - z_{l-1})}, \tilde{\psi}_2 = C_1\mathrm{e}^{\mathrm{i}\beta(z - z_{l-1})} + C_2\mathrm{e}^{-\mathrm{i}\beta(z - z_{l-1})},
\end{aligned} \tag{7}$$

where $\alpha^2 = \omega^2/a^2 - k^2$, $\beta^2 = \omega^2/b^2 - k^2$, $k^2 = k_1^2 + k_2^2$. The stresses given by Eqs. (3) in a Fourier domain can be written as follows:

$$\tilde{\sigma}_{zz} = -\frac{\lambda\omega^2}{a^2}\tilde{\phi} + 2\mu\left(\frac{\partial^2\tilde{\phi}}{\partial z^2} + \frac{\partial^3\tilde{\psi}_2}{\partial z^3}\right) + 2\rho\omega^2\frac{\partial\tilde{\psi}_2}{\partial z},$$

$$\tilde{\tau}_{xz} = 2\mathrm{i}k_1\mu\left(\frac{\partial\tilde{\phi}}{\partial z} + \frac{\partial^2\tilde{\psi}_2}{\partial z^2}\right) + \mathrm{i}k_2\mu\frac{\partial\tilde{\psi}_1}{\partial z} + \mathrm{i}\rho\omega^2 k_1\tilde{\psi}_2,$$

$$\tilde{\tau}_{yz} = 2\mathrm{i}k_2\mu\left(\frac{\partial\tilde{\phi}}{\partial z} + \frac{\partial^2\tilde{\psi}_2}{\partial z^2}\right) - \mathrm{i}k_1\mu\frac{\partial\tilde{\psi}_1}{\partial z} + \mathrm{i}\rho\omega^2 k_2\tilde{\psi}_2. \tag{8}$$

Now, the substitution of solutions (7) into Eqs. (8), results in a matrix relation written for the Fourier transforms of the displacement vector and the stresses evaluated at the top of the layer $z = z_l$ $(z_l - z_{l-1} = h_l)$

$$\begin{pmatrix} \tilde{u}_x^{(l)}(h_l) \\ \tilde{u}_y^{(l)}(h_l) \\ \tilde{u}_z^{(l)}(h_l) \\ \tilde{\sigma}_{zz}^{(l)}(h_l) \\ \tilde{\tau}_{xz}^{(l)}(h_l) \\ \tilde{\tau}_{yz}^{(l)}(h_l) \end{pmatrix} = \begin{pmatrix} g_{11}(h_l) & \dots & g_{16}(h_l) \\ \vdots & \vdots & \vdots \\ g_{61}(h_l) & \dots & g_{66}(h_l) \end{pmatrix} \begin{pmatrix} D_1 \\ D_2 \\ D_3 \\ D_4 \\ D_5 \\ D_6 \end{pmatrix},$$

or in short notation

$$\{\mathbf{V}^{(l)}(h_l)\} = [\mathbf{g}(h_l)]\{\mathbf{D}\}, \tag{9}$$

with $\{\mathbf{V}^{(l)}(h_l)\}$ the state vector, $D_{1,2} = A_1 \pm A_2$, $D_{3,4} = C_1 \pm C_2$, $D_{5,6} = B_1 \pm B_2$, respectively. The matrix $[\mathbf{g}(h_l)]$ is given in Appendix A. At the bottom of the layer $z = z_{l-1}$, another relation, similar to Eq. (9), can be obtained. At the same time, using the boundary conditions (4), one can deduce that the same relation holds at the upper surface of layer $(l-1)$

$$\{\mathbf{V}^{(l)}(0)\} = [\mathbf{g}(0)]\{\mathbf{D}\} \quad \text{with} \quad \{\mathbf{V}^{(l-1)}(h_{l-1})\} = \{\mathbf{V}^{(l)}(0)\}. \tag{10}$$

Substitution of the solution of system (10) with respect to $\{\mathbf{D}\}$ into Eq. (9) results in the matrix which connects $\tilde{u}_x^{(l)}, \dots, \tilde{\tau}_{yz}^{(l)}$ with $\tilde{u}_x^{(l-1)}, \dots, \tilde{\tau}_{yz}^{(l-1)}$ throughout the layer with number $l$

$$\{\mathbf{V}^{(l)}\} = [\mathbf{s}^{(l)}]\{\mathbf{V}^{(l-1)}\}, \tag{11}$$

where

$$[\mathbf{s}^{(l)}] = [\mathbf{g}(h_l)][\mathbf{g}(0)]^{-1},$$

the elements of matrix $[\mathbf{s}^{(l)}]$ being given in Appendix A.

Next, the index $l$ in Eq. (11) is set equal to $n$. Successive application of Eq. (11) in ascending order then leads to a relation which maps the state vector (which contains the displacement and the stresses) from the lower surface of the laminate to the top surface

$$\{\mathbf{V}^{(n)}\} = [\mathbf{S}]\{\mathbf{V}^{(0)}\}, \tag{12}$$

where $S$ is the total transfer matrix

$$[\mathbf{S}] = [\mathbf{s}^{(n)}][\mathbf{s}^{(n-1)}]\ldots[\mathbf{s}^{(1)}].$$

It should be noted here that the transfer matrix method, as indicated by some authors [12], can be prone to numerical instability especially in the case of a large number of layers. This problem, which is clearly due to finite precision of computations, can effectively be resolved using numerical libraries with arbitrary precision (such as the CLN library).

The transfer matrix will now be verified for two test cases. For the first test case an aluminum layer is considered which is stress-free at the top and which is in welded contact with an aluminum half-space (material properties are given in Appendix B). This implies that at the top of the layer

$$\tilde{\sigma}_{zz}^{(1)} = \tilde{\tau}_{xz}^{(1)} = \tilde{\tau}_{yz}^{(1)} = 0 \tag{13}$$

and that at the bottom the displacement and stresses have to be continuous, so that the state vector $\{\mathbf{V}^{(0)}\}$ is defined as

$$\{\mathbf{V}^{(0)}\} = [\mathbf{H}]\{A_1, A_2, A_3\}^{\mathrm{T}}, \tag{14}$$

where matrix [**H**] describes the half-space response (the matrix is elaborated in Appendix C). Substitution of Eqs. (13) and (14) into system (12) with subsequent rearrangement of the terms together with the condition of non-zero solutions results in an algebraic system with respect to $A_1, A_2, A_3$. The determinant of this system yields an implicit relation $D(\omega, k) = 0$ for the determination of $(\omega, k)$-pairs for the free waves propagating in the structure. In the present case, it is known that a free-wave solution exists in the form of surface or Rayleigh waves, which are non-dispersive, see the straight (dashed) line in Fig. 2. It is important to note that the graphs in Fig. 2 (and in the subsequent figures) plotted in the dimensionless co-ordinates: frequency $\Omega = \omega/\omega^*$ and wave vector $K = k/k^*$, where $\omega^* = c_0/H_0$, $k_* = 1/H_0$ and $c_0 = 1000$ m/s, $H_0 = 10^{-4}$ m are the scaling velocity and thickness, respectively.

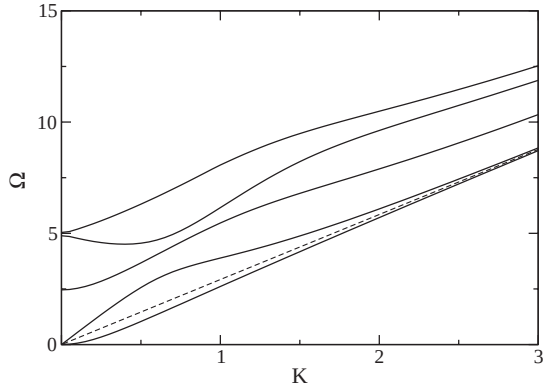


Fig. 2. Dispersion relations for the lowest modes in the aluminum layer and for Rayleigh waves in the aluminum half-space (dashed line).

For the second case, an aluminum layer in a vacuum is considered, i.e., the boundaries of the layer are stress-free. So, according to system (12)

$$\begin{aligned}
&s_{11}\tilde{u}_x^{(0)} + s_{12}\tilde{u}_y^{(0)} + s_{13}\tilde{u}_z^{(0)} = \tilde{u}_x^{(1)},\\
&s_{21}\tilde{u}_x^{(0)} + s_{22}\tilde{u}_y^{(0)} + s_{23}\tilde{u}_z^{(0)} = \tilde{u}_y^{(1)},\\
&s_{31}\tilde{u}_x^{(0)} + s_{32}\tilde{u}_y^{(0)} + s_{33}\tilde{u}_z^{(0)} = \tilde{u}_z^{(1)},\\
&s_{41}\tilde{u}_x^{(0)} + s_{42}\tilde{u}_y^{(0)} + s_{43}\tilde{u}_z^{(0)} = 0,\\
&s_{51}\tilde{u}_x^{(0)} + s_{52}\tilde{u}_y^{(0)} + s_{53}\tilde{u}_z^{(0)} = 0,\\
&s_{61}\tilde{u}_x^{(0)} + s_{62}\tilde{u}_y^{(0)} + s_{63}\tilde{u}_z^{(0)} = 0.
\end{aligned} \tag{15}$$

As in the previous example, the determinant of the last three equations results in an implicit dispersion relation for the wave modes propagating in the layer. Moreover, using the first three equations one can obtain the separate dispersion relations for the symmetric and antisymmetric modes. In doing so, it was assumed that a plane wave propagates along the $x$-co-ordinate, so that $\tilde{u}_y = 0$. Further, for the symmetric modes one may set that $\tilde{u}_x^{(1)} = \tilde{u}_x^{(0)}$, $\tilde{u}_z^{(1)} = -\tilde{u}_z^{(0)}$ and for asymmetric modes $\tilde{u}_x^{(1)} = -\tilde{u}_x^{(0)}$, $\tilde{u}_z^{(1)} = \tilde{u}_z^{(0)}$, respectively. Fig. 2 represents the results of the numerical elaboration of the dispersion relation (only the lowest modest are shown).

## 3. Solution of the thermo-elastic problem

Now turn to the problem of determining the equivalent elastic boundary conditions when the photo-thermal source is applied. Consider an isotropic elastic half-space with $z<0$. A laser beam incidents normally on the stress-free surface of the half-space. Further, it is assumed that the absorbed laser energy density is smaller than the specific heat of vaporization of the half-space material, and the thermal mechanism of sound generation is considered. The heat source is generated in the solid due to adsorbtion of the energy of the laser beam. Within the frame of the theory of thermoelastic stresses, the problem can be stated as follows [13]:

$$\begin{aligned}
&\nabla^2\phi - \frac{1}{a^2}\frac{\partial^2\phi}{\partial t^2} = m\theta, \quad \nabla^2\psi_\varepsilon - \frac{1}{b^2}\frac{\partial^2\psi_\varepsilon}{\partial t^2} = 0, \quad \varepsilon = 1, 2,\\
&\nabla^2\theta - \frac{1}{\gamma}\frac{\partial\theta}{\partial t} = -\frac{1}{\kappa}Q, \quad Q = Q_0\xi\, \mathrm{e}^{z\xi} f(\mathbf{r}, t),
\end{aligned} \tag{16}$$

where the half-space surface at $z = 0$ is stress-free and the heat flux across the solid surface is neglected:

$$\sigma_{zz} = \tau_{xz} = \tau_{yz} = 0, \quad \frac{\partial\theta}{\partial z}(\mathbf{r}, z = 0, t) = 0, \tag{17}$$

where $m = \eta(\lambda + 2\mu/3)/(\lambda + 2\mu) = \eta(3 - 4b^2/a^2)/3$ and $\eta$ is the volumetric thermal expansion coefficient, $\rho$ is the density, $c_\epsilon$ is the specific heat constant at constant strain, $\kappa$ is the thermal conductivity, $\gamma = \kappa/(\rho c_\epsilon)$ is the thermal diffusivity, $\theta = T - T_0$, $T_0$ is the reference temperature, $Q$ describes the power absorbed per unit volume, $\xi$ is the constant which is inversely proportional to the so-called skin thickness, $f(\mathbf{r}, t)$ defines the transverse and temporal distribution of the power

density in the laser beam. In the thermoelastic case the stresses in terms of the displacement components are defined as follows:

$$\sigma_{zz}^{\theta} = 2\,\mu\frac{\partial u_z}{\partial z} + (\lambda\boldsymbol{\nabla}.\mathbf{u} - (\lambda+2\mu)m\theta),$$
$$\tau_{xz}^{\theta} = \mu\left(\frac{\partial u_x}{\partial z} + \frac{\partial u_z}{\partial x}\right), \quad \tau_{yz}^{\theta} = \mu\left(\frac{\partial u_y}{\partial z} + \frac{\partial u_z}{\partial y}\right).$$

These expression can be rewritten in terms of scalar potentials $\phi$, $\psi_1$, $\psi_2$:

$$\sigma_{zz}^{\theta} = \rho\left(\frac{\partial^2\phi}{\partial t^2} - 2\frac{\partial^3\psi_2}{\partial z\partial t^2}\right) - 2\mu\left(\frac{\partial^2\phi}{\partial x^2} + \frac{\partial^2\phi}{\partial y^2} - \frac{\partial^3\psi_2}{\partial z^3}\right),$$
$$\tau_{xz}^{\theta} = 2\mu\left(\frac{\partial^2\phi}{\partial z\partial x} + \frac{\partial^3\psi_2}{\partial x\partial z^2}\right) + \mu\frac{\partial^2\psi_1}{\partial z\partial y} - \rho\frac{\partial^3\psi_2}{\partial x\partial t^2},$$
$$\tau_{yz}^{\theta} = 2\mu\left(\frac{\partial^2\phi}{\partial z\partial y} + \frac{\partial^3\psi_2}{\partial y\partial z^2}\right) - \mu\frac{\partial^2\psi_1}{\partial z\partial x} - \rho\frac{\partial^3\psi_2}{\partial y\partial t^2}, \tag{18}$$

where the temperature $\theta$ has been eliminated from $\sigma_{zz}$ using the first equation of Eqs. (16) for the potential $\phi$. In the Fourier domain (after application of Eq. (5)), Eqs. (16) and (17) yield

$$\frac{\partial^2\tilde{\phi}}{\partial z^2} + \alpha^2\tilde{\phi} = m\,\tilde{\theta}, \quad \frac{\partial^2\tilde{\psi}_\varepsilon}{\partial z^2} + \beta^2\tilde{\psi}_\varepsilon = 0, \quad \varepsilon = 1,2, \tag{19}$$

$$\frac{\partial^2\tilde{\theta}}{\partial z^2} - \chi^2\tilde{\theta} = -\frac{Q_0\xi e^{z\xi}}{\kappa}\tilde{f}(k_1,k_2,\omega), \quad \frac{\partial\tilde{\theta}}{\partial z}(k_1,k_2,z=0,\omega) = 0, \tag{20}$$

where $\chi^2 = k^2 - i\omega/\gamma$. The solution of Eqs. (20) is given by

$$\tilde{\theta} = -K_0\left(e^{\xi z} - \frac{\xi}{\chi}e^{\chi z}\right) \quad \text{with} \quad K_0 = \frac{Q_0\xi\tilde{f}(k_1,k_2,\omega)}{\kappa(\xi^2-\chi^2)}.$$

Accordingly, the solutions of Eqs. (19) read

$$\tilde{\phi} = -\frac{mK_0}{(\xi^2+\alpha^2)}e^{\xi z} + \frac{m\xi K_0}{\chi(\chi^2+\alpha^2)}e^{\chi z} + A(k_1,k_2,\omega)\,e^{-i\alpha z},$$
$$\tilde{\psi}_1 = B(k_1,k_2,\omega)\,e^{-i\beta z}, \quad \tilde{\psi}_2 = C(k_1,k_2,\omega)\,e^{-i\beta z}, \tag{21}$$

where the branches of radicals are fixed as follows $\Re(\chi) > 0$, $\Im(\alpha) > 0$, $\Im(\beta) > 0$. Substitution of these expressions into the Fourier-transformed stress conditions at the boundary $z = 0$ results in a

linear algebraic system with respect to the unknowns $A$, $B$, $C$:

$$
\begin{aligned}
&-\mu(\beta^2-k^2)A-2\,\mathrm{i}\,\mu\,\beta k^2 C+\rho m K_0\omega^2\left(\frac{1}{(\alpha^2+\xi^2)}-\frac{\xi}{\chi(\alpha^2+\chi^2)}\right)\\
&-2\mu m K_0\left(\frac{k_1^2}{(\alpha^2+\xi^2)}-\frac{\xi k_1^2}{\chi(\alpha^2+\chi^2)}+\frac{k_2^2}{(\alpha^2+\xi^2)}-\frac{\xi k_2^2}{\chi(\alpha^2+\chi^2)}\right)=0,\\
&2\mu k_1\alpha A+\mu\beta k_2 B-\mathrm{i}\mu k_1(\beta^2-k^2)C+2\mu m K_0\xi\left(\frac{\mathrm{i}k_1}{(\alpha^2+\chi^2)}-\frac{\mathrm{i}k_1}{(\alpha^2+\xi^2)}\right)=0,\\
&2\mu k_2\alpha A-\mu\beta k_1 B-\mathrm{i}\mu k_2(\beta^2-k^2)C+2\mu m K_0\xi\left(\frac{\mathrm{i}k_2}{(\alpha^2+\chi^2)}-\frac{\mathrm{i}k_2}{(\alpha^2+\xi^2)}\right)=0.
\end{aligned}
$$

Now one has to take into account that $\xi\sim 10^9\ \mathrm{m}^{-1}$, so that terms with order $1/\xi^2$ can be neglected. Thus, one arrives at the system

$$
\begin{aligned}
&-(\beta^2-k^2)A-2\mathrm{i}\beta k^2 C=mQ_0\tilde{f}(k_1,k_2,\omega)\frac{(\beta^2-k^2)}{\kappa\chi(\alpha^2+\chi^2)},\\
&2k_1\alpha A+\beta k_2 B-\mathrm{i}k_1(\beta^2-k^2)C=-2mQ_0\tilde{f}(k_1,k_2,\omega)\frac{\mathrm{i}k_1}{\kappa(\alpha^2+\chi^2)},\\
&2k_2\alpha A-\beta k_1 B-\mathrm{i}k_2(\beta^2-k^2)C=-2mQ_0\tilde{f}(k_1,k_2,\omega)\frac{\mathrm{i}k_2}{\kappa(\alpha^2+\chi^2)}.
\end{aligned}
\tag{22}
$$

An analogous system of equations can be written for the following classical elasticity problem (with stresses written in a classical form):

$$
\begin{aligned}
&\nabla^2\phi-\frac{1}{a^2}\frac{\partial^2\phi}{\partial t^2}=0,\quad \nabla^2\psi_\varepsilon-\frac{1}{b^2}\frac{\partial^2\psi_\varepsilon}{\partial t^2}=0,\quad \varepsilon=1,2,\\
&\text{at}\quad z=0:\quad \sigma_{zz}=Z(x,y,t),\quad \tau_{xz}=X(x,y,t),\quad \tau_{yz}=Y(x,y,t).
\end{aligned}
\tag{23}
$$

In the Fourier domain the problem described by Eqs. (23) leads to the following algebraic system:

$$
\begin{aligned}
&-(\beta^2-k^2)A-2\mathrm{i}k^2\beta C=\tilde{Z}(k_1,k_2,\omega)/\mu,\\
&2k_1\alpha A+\beta k_2 B-\mathrm{i}k_1(\beta^2-k^2)C=\tilde{X}(k_1,k_2,\omega)/\mu,\\
&2k_2\alpha A-\beta k_1 B-\mathrm{i}k_2(\beta^2-k^2)C=\tilde{Y}(k_1,k_2,\omega)/\mu.
\end{aligned}
\tag{24}
$$

Clearly, the left-hand of Eqs. (22) and (24) are identical. Thus, the right-hand of Eqs. (22) can be interpreted as a Fourier image of the equivalent stresses applied at the boundary. So, under the following assumptions which were made implicitly: (a) the heating is localized within a very thin layer of the top layer of the laminate, (b) the thermo-diffusion depth is small compared to the thickness of layer (i.e., half-space space can be used instead of layer, (c) the exposition time of the laser is relatively short and (d) thermal radiation losses from the surface can be neglected, the laser or photothermal source may be represented as an equivalent elastic boundary source consisting of distributed normal and shear loading boundary conditions. Similar boundary equivalent conditions were found by Spicer [14] and they were also used in Ref. [6]. It should be noted that the same boundary conditions can be obtained if one specifies the heat flux at the boundary instead of the heat source.

From Eqs. (22) it can be concluded that equivalent boundary conditions in the space–time domain are presented by the convolution integral

$$\sigma_{jz}(x,y,t) = \int\int\int K_j(\mathbf{r}-\bar{\mathbf{r}}, t-\tau) f(\bar{\mathbf{r}},\tau)\,\mathrm{d}\bar{\mathbf{r}}\,\mathrm{d}\tau, \quad j = z,x,y. \tag{25}$$

The kernels $K_j(\mathbf{r},t)$ are functions of time and the co-ordinates depend on the properties of the body. They can be found by the substitution $f(\bar{\mathbf{r}},\tau) = \delta(\tau)\delta(\bar{\mathbf{r}})$. In doing so, one arrives at the following expressions for $K_x$ and $K_y$:

$$K_x = -2\Gamma_0 \frac{\partial}{\partial x}\delta(\mathbf{r})\vartheta(t), \quad K_y = -2\,\Gamma_0 \frac{\partial}{\partial y}\delta(\mathbf{r})\vartheta(t), \tag{26}$$

where

$$\vartheta(t) = \begin{cases} \mathrm{e}^{a^2 t/\gamma}, & t<0, \\ 1, & t>0, \end{cases}$$

and $\Gamma_0 = Q_0 b^2 m/c_\epsilon$. As can be understood from general considerations, the value of the equivalent stresses can depend only on the values of the "thermo-force" $f$ at previous times and not at subsequent times (the causality principle), so that Eq. (25) must be rewritten in the form

$$\sigma_{jz}(x,y,t) = \int_{-\infty}^{t} \int\int K_j(\mathbf{r}-\bar{\mathbf{r}}, t-\tau) f(\bar{\mathbf{r}},\tau)\,\mathrm{d}\bar{\mathbf{r}}\,\mathrm{d}\tau, \quad j = z,x,y. \tag{27}$$

However, Eq. (26) still violates the causality principle, since the stresses (effect) appear for negative $t$, i.e., before the cause—a laser impulse. This appears as a consequence of the non-limited speed of the heat propagation. The problem can be solved by letting $\vartheta(t) = \mathrm{h}(t)$, where $\mathrm{h}(t)$ is the Heaviside step-function. This leads to the following Fourier images of the kernels:

$$\tilde{K}_z = \mathrm{i}\,\Gamma_0 \frac{(\beta^2 - k^2)}{\omega\sqrt{k^2 - \mathrm{i}\,\omega/\gamma}}, \quad \tilde{K}_x = 2\,\Gamma_0 \frac{k_1}{\omega}, \quad \tilde{K}_y = 2\Gamma_0 \frac{k_2}{\omega}, \tag{28}$$

which subsequently results in the following expressions in time–space domain (for details see Appendix D):

$$K_z = -\Gamma_0 h(t)\left(\frac{1}{b^2}\frac{\partial^2}{\partial t^2} - 2\,\Delta_\perp\right)\left(\frac{1}{2\pi r}\left(1 - \Phi\left(\frac{r}{2\sqrt{\gamma t}}\right)\right)\right),$$

$$K_x = -2\Gamma_0 \mathrm{h}(t)\frac{\partial}{\partial x}\delta(\mathbf{r}), \quad K_y = -2\,\Gamma_0\,\mathrm{h}(t)\frac{\partial}{\partial y}\delta(\mathbf{r}), \tag{29}$$

where $\Delta_\perp = \partial_x^2 + \partial_y^2$ and $\Phi(..)$ is the error function. It should be noted that Eqs. (29) have to be understood in the sense of distributions [15]. The obtained results for $K_{(x,y)}$ are similar to those derived by Rose [16]. However, using the dipole approach that was used in Ref. [16], one obtains that $K_z = 0$, which is apparently due to the limitations of the method. A more rigorous derivation of the corrected stress expressions with respect to non-causality problem can be done using relations similar to the Kramer–Kronig relations that express the relations between real and imaginary parts of the susceptibility function [17].

## 4. Moving photo-thermal source

Consider a laser beam, which is scanning uniformly with a constant speed $V$ along the surface of the laminate. The power intensity of the beam is monochromatically modulated with the modulation frequency $\Omega_0$. Then, the heat source generated in the top layer can written as

$$Q = 0.5I_0(1 + \exp(-\mathrm{i}\Omega_0 t))\xi \mathrm{e}^{z\xi}\frac{1}{\pi l^2}\mathrm{e}^{-\frac{(x-Vt)^2+y^2}{l^2}}, \tag{30}$$

where it was assumed that the laser beam has a total power intensity $I_0$ and that the spot radius $l$ has a Gaussian spatial distribution of power intensity. According to the previous subsection, in the Fourier-domain this heat source is equivalent to the following distributed stresses applied at the surface (the superscript $\theta$ indicates that these stresses are thermal stresses):

$$\tilde{\sigma}^{\theta}_{zz} = \Delta\frac{\mathrm{i}(\beta^2 - k^2)}{\omega\sqrt{k^2 - \mathrm{i}\omega/\eta}}, \quad \tilde{\tau}^{\theta}_{xz} = 2\Delta\frac{k_1}{\omega}, \quad \tilde{\tau}^{\theta}_{yz} = 2\,\Delta\frac{k_1}{\omega}, \tag{31}$$

where

$$\Delta = \frac{\pi b^2 m I_0}{c_\varepsilon}\mathrm{e}^{-\frac{k^2 l^2}{4}}(\delta(\omega - k_1 V) + \delta(\omega - k_1 V - \Omega_0)).$$

Also assume that the lower boundary of the laminate is in stiff contact with an elastic substrate which occupies the lower half-space. The goal is to find the $z$-component of the top layer displacement, which can be measured in principle and used further by, for instance, the Fabry-Perot interferometer [18].

The laminate response is described by matrix (12) which has to be supplied with proper boundary conditions at the half-space interface

$$[\mathbf{S}]\{\mathbf{V}^{(0)}\} = \{\mathbf{V}^{(n)}\} \quad \text{with} \quad \{\mathbf{V}^{(0)}\} = [\mathbf{H}]\{A_1, A_2, A_3\}^{\mathrm{T}}, \tag{32}$$

where the stresses in the state vector $\{\mathbf{V}^{(n)}\}$ are given by Eq. (31) and the matrix $[\mathbf{H}]$ is given in Appendix C. So one arrives at the system

$$\begin{pmatrix} \tilde{u}^{(n)}_x \\ \tilde{u}^{(n)}_y \\ \tilde{u}^{(n)}_z \\ \tilde{\sigma}^{\theta}_{zz} \\ \tilde{\tau}^{\theta}_{xz} \\ \tilde{\tau}^{\theta}_{yz} \end{pmatrix} = \begin{pmatrix} k_{11} & k_{12} & k_{13} \\ k_{21} & k_{22} & k_{23} \\ k_{31} & k_{32} & k_{33} \\ k_{41} & k_{42} & k_{43} \\ k_{51} & k_{52} & k_{53} \\ k_{61} & k_{62} & k_{63} \end{pmatrix} \begin{pmatrix} A_1 \\ A_2 \\ A_3 \end{pmatrix},$$

where $k_{ij} = s_{ik}h_{kj}$. The last three equations can be solved with respect to the unknowns $A_1, A_2, A_3$, which, in turn, can be used for the determination of the unknown $\tilde{u}^{(n)}_i$. Finally, the $z$-component of

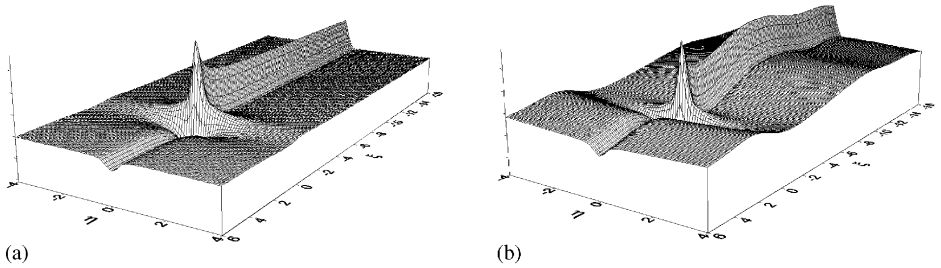

(a) (b)

Fig. 3. Normal displacements of the laminate bonded to a steel half-space due to uniformly moving laser $V = 2.7, \Omega_0 = 0.0$, the laminate consist of (a) 1 aluminum layer. (b) 5 alternating layers aluminum + resin.

the top layer displacement can be written using the following inverse Fourier form:

$$u_z(x - Vt, y, t) = \int\int F(k_1, k_2, \omega = k_1 V) e^{i(k_1(x-Vt)+k_2 y)}\, dk_1\, dk_2 + \int\int F(k_1, k_2, \omega = k_1 V + \Omega_0) e^{i(k_1(x-Vt)+k_2 y - i\,\Omega_0\, t)}\, dk_1\, dk_2. \quad (33)$$

The results of the numerical evaluation of the integral in Eq. (33) for the different problem parameters are shown in Fig. 3.

As seen in Fig. 3(a), the laser spot excites the steady state displacement field in the laminate. These displacements appear as a result of the thermal expansion of the laminate material which is heated by the laser. Also, it is seen that no waves are generated. When the structure becomes more complex (5 layers), the laser spot when moving at the same speed, generates waves in the laminate, see Fig. 3(b). Note that the graphs have been plotted in the dimensionless co-ordinates: $\zeta = (x - Vt)/H_0$, $\eta = y/H_0$. These results can be understood qualitatively using the following arguments. The zeros of the denominator of the integrand of Eq. (33) that correspond to the wave dispersion of the system, can be found from the system

$$\omega = \mathbf{k} \cdot \mathbf{V} + \Omega_0,$$

$$D(k_1, k_2, \omega) = 0,$$

where the first equation is the so-called kinematic invariant and the second is the implicit dispersion relation of the system, i.e., the denominator of the integrand in Eq. (33). A graphical solution of the system is shown in Fig. 4.

Fig. 4(a) shows that in this case there are no crossing points between the kinematic invariant and the dispersion curves (except for $\omega = 0, k = 0$) and thus no waves are generated in the system. In contrast, Fig. 4(b) shows that there are crossing points and therefore waves are generated by the moving laser spot.

It is clear that the dispersion properties of the combined system strongly depend on the properties of the bounded half-space. This can be confirmed by the graphs shown in Fig. 5, where a polyester resin half-space was used instead of a steel half-space. As shown in Fig. 5, in this case

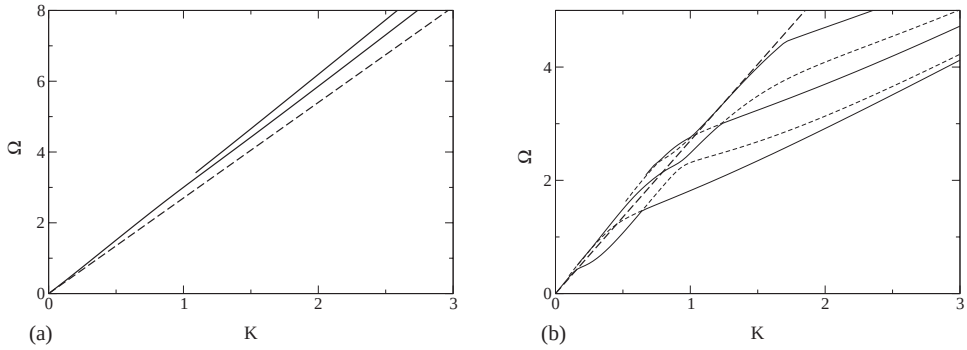


Fig. 4. Dispersion curves of laminated structure bonded to a steel half-space with kinematic invariant $V = 2.7, \Omega_0 = 0.$, the structure consist of (a) 1 aluminum layer, (b) 5 alternating layers aluminum + prepreg (- - - kinematic invariant).

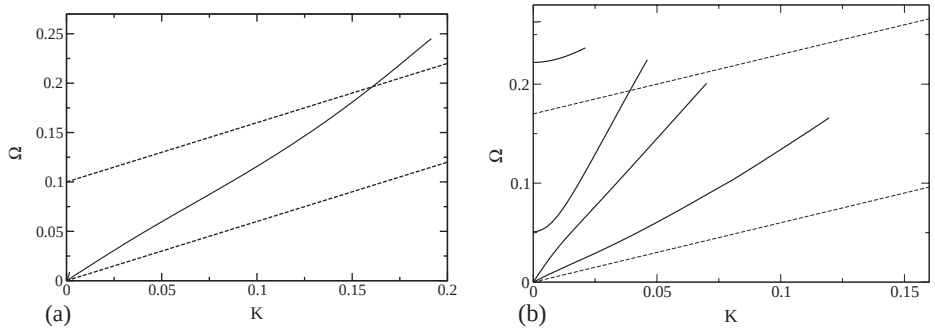


Fig. 5. Dispersion curves of laminated structure bonded to a polyester resin half-space with kinematic invariant, the structure consist of (a) 1 aluminum layer $V = 1.1, \Omega_0 = 0.02$, (b) 5 alternating layers aluminum + prepreg $V = 0.6, \Omega_0 = 0.17$ (- - - kinematic invariant).

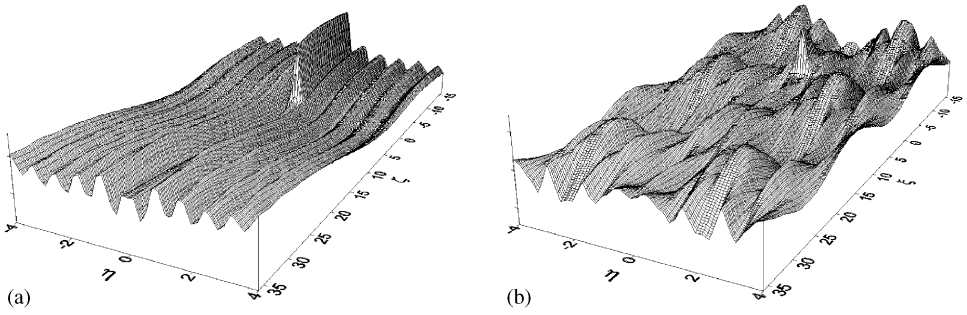


Fig. 6. Normal displacements of the laminate bonded to a polyester resin half-space due to uniformly moving laser, the laminate consist of (a) 1 aluminum layer $V = 1.1, \Omega_0 = 0.02$, (b) 5 alternating layers aluminum + resin $V = 0.6, \Omega_0 = 0.17$.

each mode can be excited separately, which can be useful in NDE applications. The corresponding spatial displacement fields are shown in Fig. 6.

The displacement field shown in Fig. 6 appears to be quite complicated and also it differs substantially from the fields generated, for instance, by moving mechanical loads [19]. In particular, the displacement field generated by a moving mechanical load is localized in the

vicinity of the load (sub-critical case). In the thermoelastic case, the field extends over some distance away from the laser spot, because of the temperature relaxation processes.

## 5. Conclusions

In the present paper, the steady state response of an elastic isotropic layered plate subjected to a moving laser source illumination has been studied. The response of the layered plate in Fourier domain has been formulated using the transfer matrix approach. The application of the photo-thermal source (laser) to the upper surface of the laminate, has been reformulated as equivalent stresses applied at the illuminated boundary with the use of the so-called *thermal stresses* approximation. For the analysis a laminated structure has been used which consists of alternating layers of aluminum and so-called prepreg (usually, fiber-reinforced resin or epoxy) which is used in the aerospace industry. The sensitivity of the generated displacement field to the variations of the laminate inner structure has been demonstrated. The model provides a useful tool for the determination of which modes are generated by a laser source in a layered system. It can also be used to determine how sensitive the generated modes are to changes in density, thickness, or elastic properties of the layers. Future work will focus on the analysis of different laws of motion of the laser spot in order to obtain an optimal radiation pattern which can be used further to determine the properties of layered structures using an inverse method.

## Appendix A

The matrix $[\mathbf{g}(h_l)]$ is given by

$$\begin{pmatrix} \mathrm{i}k_1 c_a & -k_1 s_a & \mathrm{i}k_2 c_b & -k_2 s_b & -\mathrm{i}k_1\beta s_b & -k_1\beta c_b \\ \mathrm{i}k_2 c_a & -k_2 s_a & -\mathrm{i}k_1 c_b & k_1 s_b & -\mathrm{i}k_2\beta s_b & -k_2\beta c_b \\ -\alpha s_a & \mathrm{i}\alpha c_a & 0 & 0 & k^2 c_b & \mathrm{i}k^2 s_b \\ -\mu\delta^2 c_a & -\mathrm{i}\mu\delta^2 s_a & 0 & 0 & -2\mu\beta k^2 s_b & 2\mathrm{i}\mu\beta k^2 c_b \\ -2\mathrm{i}\mu k_1\alpha s_a & -2\mu k_1\alpha c_a & -\mathrm{i}\mu k_2\beta s_b & -\mu k_2\beta c_b & -\mathrm{i}\mu\, k_1\delta^2 c_b & \mu k_1\delta^2 s_b \\ -2\mathrm{i}\mu k_2\alpha s_a & -2\mu k_2\alpha c_a & \mathrm{i}\mu k_1\beta s_b & \mu k_1\beta c_b & -\mathrm{i}\mu k_2\delta^2 c_b & \mu k_2\delta^2 s_b \end{pmatrix},$$

where $c_a = \cos(\alpha h_l)$, $c_b = \cos(\beta h_l)$, $s_a = \sin(\alpha h_l)$, $s_b = \sin(\beta h_l)$, $\delta^2 = \beta^2 - k^2$, $k^2 = k_1^2 + k_2^2$. The matrix $[\mathbf{g}(0)]$ can be obtained by letting $h_l = 0$ in matrix $[\mathbf{g}(h_l)]$, so that

$$[\mathbf{g}(0)] = \begin{pmatrix} \mathrm{i}k_1 & 0 & \mathrm{i}k_2 & 0 & 0 & -k_1\beta \\ \mathrm{i}k_2 & 0 & -\mathrm{i}k_1 & 0 & 0 & -k_2\beta \\ 0 & \mathrm{i}\alpha & 0 & 0 & k^2 & 0 \\ -\mu\delta^2 & 0 & 0 & 0 & 0 & 2\mathrm{i}\mu\beta k^2 \\ 0 & -2\mu k_1\alpha & 0 & -\mu k_2\beta & -\mathrm{i}\mu k_1\delta^2 & 0 \\ 0 & -2\mu k_2\alpha & 0 & \mu k_1\beta & -\mathrm{i}\mu k_2\delta^2 & 0 \end{pmatrix}.$$

The inversion of this matrix results in the following matrix:

$$[\mathbf{g}(0)]^{-1} = \begin{pmatrix} \frac{-2ik_1}{W} & \frac{-2ik_2}{W} & 0 & -\frac{1}{\mu W} & 0 & 0 \\ 0 & 0 & \frac{-i\delta^2}{W\alpha} & 0 & -\frac{k_1}{\mu\alpha W} & -\frac{k_2}{\mu\alpha W} \\ \frac{-ik_2}{k^2} & \frac{ik_1}{k^2} & 0 & 0 & 0 & 0 \\ 0 & 0 & 0 & 0 & -\frac{k_2}{\mu\beta k^2} & \frac{k_1}{\mu\beta k^2} \\ 0 & 0 & \frac{2}{W} & 0 & \frac{ik_1}{\mu W k^2} & \frac{ik_2}{\mu W k^2} \\ \frac{-k_1\delta^2}{\beta k^2 W} & \frac{-k_2\delta^2}{\beta k^2 W} & 0 & \frac{-i}{\mu\beta W} & 0 & 0 \end{pmatrix},$$

where $W = \omega^2/b^2$. According to the definition

$$[\mathbf{s}^{(l)}] = [\mathbf{g}(h_l)][\mathbf{g}(0)]^{-1}.$$

This, after elaboration, results in the following relation:

$$[\mathbf{s}^{(l)}] = \frac{1}{W}[\mathbf{q}^{(l)}],$$

where the elements of the auxiliary matrix $[\mathbf{q}^{(l)}]$ are (index $l$ omitted)

$$q_{11} = Wc_b + 2k_1^2(c_a - c_b), q_{12} = 2k_1k_2(c_a - c_b), q_{13} = ik_1\left(\delta^2\frac{s_a}{\alpha} - 2\beta s_b\right),$$

$$q_{14} = -i\frac{k_1}{\mu}(c_a - c_b), q_{15} = W\frac{s_b}{\mu\beta} + \frac{k_1^2}{\mu}\left(\frac{s_a}{\alpha} - \frac{s_b}{\beta}\right), q_{16} = \frac{k_1k_2}{\mu}\left(\frac{s_a}{\alpha} - \frac{s_b}{\beta}\right),$$

$$q_{21} = q_{12}, q_{22} = Wc_b + 2k_2^2(c_a - c_b), q_{23} = ik_2\left(\delta^2\frac{s_a}{\alpha} - 2\beta s_b\right),$$

$$q_{24} = -i\frac{k_2}{\mu}(c_a - c_b), q_{25} = q_{16}, q_{26} = W\frac{s_b}{\mu\beta} + \frac{k_2^2}{\mu}\left(\frac{s_a}{\alpha} - \frac{s_b}{\beta}\right),$$

$$q_{31} = ik_1\left(2\alpha s_a - \delta^2\frac{s_b}{\beta}\right), q_{32} = ik_2\left(2\alpha s_a - \delta^2\frac{s_b}{\beta}\right),$$

$$q_{33} = Wc_a + 2k^2(c_b - c_a), q_{34} = \frac{1}{\mu}\left(\frac{k^2 s_b}{\beta} + \alpha s_a\right), q_{35} = q_{14}, q_{36} = q_{24},$$

$$q_{41} = 2i\mu k_1\delta^2(c_a - c_b), q_{42} = 2i\mu k_2\delta^2(c_a - c_b),$$

$$q_{43} = -\mu\left(4\beta k^2 s_b + \delta^4\frac{s_a}{\alpha}\right), q_{44} = q_{33}, q_{45} = q_{13}, q_{46} = q_{23},$$

$$q_{51} = -\mu\left(((\beta^2 - k_1^2)^2 + k_2^2(\beta^2 + k_1^2))\frac{s_b}{\beta} + 4k_1^2\alpha s_a\right),$$

$$q_{52} = -\mu k_1k_2\left((k^2 - 3\beta^2)\frac{s_b}{\beta} + 4\alpha s_a\right), q_{53} = q_{41}, q_{54} = q_{31}, q_{55} = q_{11}, q_{56} = q_{12},$$

$$q_{61} = q_{52}, q_{62} = -\mu\left(((\beta^2 - k_2^2)^2 + k_1^2(\beta^2 + k_2^2))\frac{s_b}{\beta} + 4k_2^2\alpha s_a\right), q_{63} = q_{42},$$

$$q_{64} = q_{32}, q_{65} = q_{12}, q_{66} = q_{22}.$$

It must be emphasized that in all the final results such as expressions for the displacement components or dispersion relations, $W$ is not included (since it mutually cancelled), hence it was assumed that

$$[\mathbf{s}^{(l)}] \equiv [\mathbf{q}^{(l)}].$$

## Appendix B

The following material constants were used in the paper:

| Material | Density ($\frac{kg}{m^3}$) | Long. vel. ($\frac{m}{s}$) | Shear vel. $\frac{m}{s}$ | Layer thick. ($m.$) |
|---|---|---|---|---|
| Aluminum | 2790 | 6380 | 3130 | $4 \times 10^{-4}$ |
| Steel | 7700 | 5760 | 3120 | $\infty$ |
| Prepreg | 1400 | 2730 | 1300 | $3 \times 10^{-4}$ |
| Polyester resin | 800 | 2550 | 1280 | $\infty$ |

Thermal diffusivity $\gamma$ for aluminum is taken as $\gamma \approx 1.0 \times 10^{-5}$ ($\frac{m^2}{s}$).

## Appendix C

In the half-space $z<0$ the scalar potentials can be written in the down-going wave form

$$\tilde{\phi} = A_1 \mathrm{e}^{-\mathrm{i}\alpha z}, \quad \tilde{\psi}_1 = A_2 \mathrm{e}^{-\mathrm{i}\beta z} \quad \tilde{\psi}_2 = A_3 \mathrm{e}^{-\mathrm{i}\beta z}.$$

Consequently, these potentials lead to the following form of the state vector evaluated at $z = 0$:

$$\{\mathbf{V}^{(0)}\} = \begin{pmatrix} \mathrm{i}k_1 & \mathrm{i}k_2 & k_1\beta \\ \mathrm{i}k_2 & -\mathrm{i}k_1 & k_2\beta \\ -\mathrm{i}\alpha & 0 & k^2 \\ -\mu\delta^2 & 0 & 2\mathrm{i}\mu\beta k^2 \\ 2\mu k_1\alpha & \mu k_2\beta & -\mathrm{i}\mu k_1\delta^2 \\ 2\mu k_2\alpha & -\mu k_1\beta & -\mathrm{i}\mu k_2\delta^2 \end{pmatrix} \begin{pmatrix} A_1 \\ A_2 \\ A_3 \end{pmatrix}.$$

## Appendix D

The inverse Fourier transform for $\tilde{K}_x$ and $\tilde{K}_y$ can be found without difficulties. However, the same operation for $\tilde{K}_z$ is not so obvious. Consider the following integral

$$K_z(r,t) = \frac{1}{8\pi^3} \int\int\int \tilde{K}_z \, \mathrm{e}^{\mathrm{i}(\mathbf{k}\,\mathbf{r}-\omega t)} \, \mathrm{d}\omega \, \mathrm{d}\mathbf{k},$$

in which

$$\tilde{K}_z = \mathrm{i}\,\Gamma_0 \frac{(\beta^2 - k^2)}{\omega\sqrt{k^2 - \mathrm{i}\,\omega/\gamma}} = \frac{\mathrm{i}\,\Gamma_0}{\sqrt{\gamma}} \frac{(\omega^2/b^2 - 2\,k^2)}{\omega\sqrt{k^2/\gamma - \mathrm{i}\,\omega}}.$$

This integral diverges in a classical sense. However, it can be treated in the sense of distributions, so that

$$K_z(r,t) = -\frac{\mathrm{i}\Gamma_0}{8\pi^3\sqrt{\gamma}}\left(\frac{1}{b^2}\frac{\partial^2}{\partial t^2} - 2\,\Delta_\perp\right) \int\int\int \frac{\mathrm{e}^{\mathrm{i}(\mathbf{k}\,\mathbf{r}-\omega t)}}{\omega\sqrt{k^2/\gamma - \mathrm{i}\omega}}\,\mathrm{d}\omega\,\mathrm{d}\mathbf{k}.$$

Next, consider the internal integral

$$I_0 = \int_{-\infty}^{+\infty} \frac{\mathrm{e}^{-\mathrm{i}\,\omega t}}{\omega\sqrt{g - \mathrm{i}\omega}}\,\mathrm{d}\,\omega \quad \text{with} \quad g = k^2\gamma.$$

The integral can be evaluated using the method of contour integration. The contour of integration for $t > 0$ is shown in Fig. 7.

For $t < 0$, the contour of integration should be closed in the upper half-plane, where there are no singular points ($I_0 = 0$). The branch cut in the complex plane $\omega$ in chosen such that the condition $\Re(\sqrt{k^2/\gamma - \mathrm{i}\omega}) = \Re(\chi) > 0$ is satisfied everywhere along the path. The contour integration gives

$$I_0 = \begin{cases} 0, & t < 0, \\ -\frac{2\pi\mathrm{i}}{\sqrt{g}} + 2\mathrm{i}\mathrm{e}^{(-gt)} \int_0^{+\infty} \dfrac{\mathrm{e}^{(-zt)}}{\sqrt{z}(z+g)}\,\mathrm{d}\,z, & t > 0, \end{cases}$$

where the remaining integral is standard,

$$I_0 = \begin{cases} 0, & t < 0, \\ -\frac{2\pi\mathrm{i}}{\sqrt{g}}\,\Phi(\sqrt{tg}), & t > 0. \end{cases}$$

Accordingly, the next integral is

$$I_1 = \int\int_{-\infty}^{+\infty} \frac{\Phi(\sqrt{k_1^2 + k_2^2}\sqrt{t\gamma})}{\sqrt{k_1^2 + k_2^2}}\,\mathrm{e}^{\mathrm{i}(k_1 x + k_2 y)}\,\mathrm{d}k_1\,\mathrm{d}k_2,$$

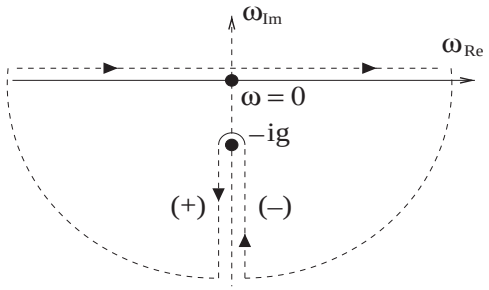


Fig. 7. Contour of integration for $t > 0$ in complex $\omega$-plane, (+) and (−) show signs of the radical, respectively.

which, in a polar system of co-ordinates: $k_1 = k\cos(\phi)$, $k_1 = k\sin(\phi)$, $x = r\sin(\psi)$, $y = r\sin(\psi)$, after integration over $\phi$, is simplified to

$$I_1 = 2\pi \int_0^{+\infty} \mathrm{J}_0(kr)\Phi(k\sqrt{t\gamma})\,\mathrm{d}k,$$

where $\mathrm{J}_0(..)$ is the Bessel function of the first kind. The last integral can be found in the standard integration tables

$$I_1 = \frac{2\pi}{r}\left(1 - \Phi(\frac{r}{2\sqrt{\gamma t}})\right).$$

Finally,

$$K_z = -\Gamma_0\,\mathrm{h}(t)\left(\frac{1}{b^2}\frac{\partial^2}{\partial t^2} - 2\,\Delta_\perp\right)\left(\frac{1}{2\pi r}\left(1 - \Phi\left(\frac{r}{2\sqrt{\gamma t}}\right)\right)\right).$$

## References


[1] C.B. Scruby, L.E. Drain, Laser Ultrasonics: Techniques and Applications, Adam Hilger, Bristol, 1990.
[2] Y. Hayashi, S. Ogawa, H. Cho, M. Takemoto, Non-contact estimation of thickness and elastic properties of metallic foils by the wavelet transform of laser-generated lamb waves, NDT& E International 32 (1999) 21–27.
[3] D.A. Hutchins, C.B. Scruby, R.J. Dewhurst, S.B. Palmer, in: R.S. Sharpe (Ed.), Research Techniques in Nondestructive testing, Vol. 5, Academic Press, New York, 1982.
[4] M.L. Lyamshev, Vibrations of a thin bounded plate excited by modulated laser radiation, Acoustical Physics 46 (6) (2000) 743–745.
[5] S. Dufang, W. Yaping, H. Yulong, Study of the directivity of laser generated ultrasound in solids, Journal of Applied Physics 83 (3) (1998) 1207–1212.
[6] T.W. Murray, A. Cheng, J.D. Achenbach, Simulation of laser-generated ultrasonic waves in layered plates, Journal of the Acoustical Society of America 110 (2) (2001) 848–855.
[7] L.M. Lyamshev, L.V. Sedov, Optical generation of sound in a liquid: thermal mechanism (review), Soviet Physics: Acoustics 27 (1) (1981) 4–18.
[8] Y.H. Berthelot, I.J. Busch-Vishniac, Thermoacoustic radiation of sound by a moving laser source, Journal of the Acoustical Society of America 81 (2) (1987) 317–327.
[9] E.A. Skelton, J.H. James, Acoustics of anisotropic planar layered media, Journal of Sound and Vibration 151 (1) (1992) 157–174.
[10] L.M. Brekhovskikh, Waves in Layered Media, Academic Press, New York, 1980.
[11] P. Morse, H. Feshbach, Methods of Theoretical Physics, McGraw-Hill, New York, 1953.
[12] A. Mal, et al., Wave propagation in layered composite laminates under periodic surface loads, Wave Motion 10 (1988) 257.
[13] W. Nowacki, Dynamics Problems of Thermoelasticity, Noordhoff, Leiden, 1975.
[14] J.B. Spicer, Laser Ultrasonics in Finite Structures: Comprehensive Modeling with Supporting Experiment, Ph.D. Thesis, Johns Hopkins University, Baltimore, MD, 1991.
[15] V. Vladimirov, Equations of Mathematical Physics, Marcel Dekker, New York, 1971.
[16] L.R.F. Rose, Point-source representation for laser-generated ultrasound, Journal of the Acoustical Society of America 75 (3) (1984) 723.
[17] L. Landau, E. Lifshitz, Electrodynamics of Continuous Media, Pergamon Press, Oxford, 1975.
[18] J. Monchalin, A. Cand, X. Jia, Detection of in-plane and out-of-plane ultrasonic displacements by a two-channel confocal fabry-perot interferometer, Applied Physics Letters 64 (4) (1994) 414–416.
[19] A. Kononov, R. Wolfert, Load motion along a beam on a viscoelastic half-space, European Journal of Mechanics A/Solids 19 (2000) 361–371.